EFFECTS OF LOCAL VERSUS SYSTEMIC ADMINISTRATION OF CXCR4 INHIBITOR
AMD3100 ON ORTHODONTIC TOOTH MOVEMENT IN RATS

Miss Narubhorn Ongprakobkul

จุฬาลงกรณ์มหาวิทยาลัย
CHULALONGKORN UNIVERSITY

A Dissertation Submitted in Partial Fulfillment of the Requirements
for the Degree of Doctor of Philosophy in Orthodontics
Department of Orthodontics
FACULTY OF DENTISTRY
Chulalongkorn University
Academic Year 2021

ผลของการฉีดยา AMD3100 เฉพาะตำแหน่ง เปรียบเทียบกับการฉีดยาแบบทั่วร่างกาย ต่อการเคลื่อนฟันทางทันตกรรมจัดฟันในหนู

น.ส.นฤพร องค์ประกอบกุล

Thesis Title	EFFECTS OF LOCAL VERSUS SYSTEMIC ADMINISTRATION OF CXCR4 INHIBITOR AMD3100 ON ORTHODONTIC TOOTH MOVEMENT IN RATS
By	Miss Narubhorn Ongprakobkul
Field of Study	Orthodontics
Thesis Advisor	Associate Professor SIRIMA PETDACHAI, D.D.S., Ph.D.

Accepted by the FACULTY OF DENTISTRY, Chulalongkorn University in Partial Fulfillment of the Requirement for the Doctor of Philosophy

.... Dean of the FACULTY OF DENTISTRY

(Professor Pornchai Jansisyanont, D.D.S., M.S., Ph.D.)

DISSERTATION COMMITTEE

.... Chairman

(Professor Emeritus Dhirawat Jotikasthira, D.D.S., M.D.Sc.)

.... Thesis Advisor

(Associate Professor SIRIMA PETDACHAI, D.D.S., Ph.D.)

.... Examiner

(Professor Keiji Moriyama, D.D.S., Ph.D.)

.... Examiner

(Professor Ikuko Morio, D.D.S., Ph.D.)

.... Examiner

(SIRICHOM SATRAWAHA, D.D.S., Ph.D.)

นฤพร องค์ประกอบกุล : ผลของการฉีดยา AMD3100 เฉพาะตำแหน่ง เปรียบเทียบกับการฉีดยา แบบทั่วร่างกาย ต่อการเคลื่อนฟันทางทันตกรรมจัดฟันในหนู. (EFFECTS OF LOCAL VERSUS SYSTEMIC ADMINISTRATION OF CXCR4 INHIBITOR AMD3100 ON ORTHODONTIC TOOTH MOVEMENT IN RATS) อ.ที่ปรึกษาหลัก : รศ. ทพญ. ดร.ศิริมา เพ็ชรดาชัย

คีโมไคน์ (chemokine) มีบทบาทสำคัญในการเคลื่อนฟันทางทันตกรรมจัดฟัน ผ่านกระบวนการการ สลายกระดูกโดยเซลล์สลายกระดูก (osteoclast) แต่อย่างไรก็ตาม กลไกพื้นฐานยังไม่ชัดเจน ดังนั้นการวิจัยนี้จึง มีวัตถุประสงค์เพื่อศึกษาผลของการฉีดยาเอเอ็มดี 3100 (AMD3100) ซึ่งต้านการจับของตัวรับคีโมไคน์ชนิดที่ 4 (CXCR4) แบบเฉพาะตำแหน่ง เปรียบเทียบกับการฉีดยาแบบทั่วร่างกาย ต่อการเคลื่อนฟันทางทันตกรรมจัดฟัน ในหนู โดยเคลื่อนฟันกรามบนขวาซี่ที่ 1 ของหนูมาทางด้านหน้า ด้วยสปริงชนิดนิกเกิลไททาเนียมขนาดแรง 10 กรัม ทำการฉีดยาทุก ๆ วันเว้นวัน โดยที่กลุ่มควบคุมได้รับการฉีดน้ำเกลือชนิดฟอสเฟตบัฟเฟอร์ ในขณะที่กลุ่มฉีด ยาเอเอ็มดี 3100 เฉพาะตำแหน่งและฉีดยาแบบทั่วร่างกาย ได้รับการฉีดบริเวณเพดานปากและกระพุ้งแก้ม และ ฉีดยาชั้นใต้ผิวหนัง ตามลำดับ ทำการวัดระยะทางการเคลื่อนฟันและกระดูกรอบฟันกรามบนขวาซี่ที่ 1 ด้วย เอกซเรย์คอมพิวเตอร์ และการวิเคราะห์ทางจุลกายวิภาค วัดปริมาณเซลล์สลายกระดูกด้วยการย้อมด้วยกรดฟอส ฟาเตสที่ทนต่อทาร์เทรต (TRAP) วัดการสะสมของคาเทปซินเค (cathepsin K) และ สโตรมอลเซลล์ดีไรฟ์แฟก เตอร์-1 (stromal cell-derived factor-1 หรือ SDF-1) ด้วยอิมมูโนฮิสโตเคมี วัดปริมาณ cathepsin K, รันซ์2 (Runx2), SDF-1, CXCR4, RANKL และ OPG ด้วยปฏิกิริยาลูกโซ่พอลิเมอเรสแบบย้อนกลับ (Reverse transcriptase polymerase chain reaction) ผลการศึกษาพบว่า ระยะทางการเคลื่อนฟันและปริมาณเซลล์ สลายกระดูกลดลงอย่างมีนัยสำคัญในกลุ่มฉีดยาเฉพาะตำแหน่งและฉีดยาแบบทั่วร่างกาย เมื่อเปรียบเทียบกับ กลุ่มควบคุม ในขณะที่ไม่มีความแตกต่างกันทางสถิติระหว่างกลุ่มทดลอง การฉีดยาเฉพาะตำแหน่งสามารถยับยั้ง การเคลื่อนที่เฉพาะฟันกราม ในขณะที่ไม่ยับยั้งการเคลื่อนที่ของฟันหน้า นอกจากนี้ยังพบว่า ความหนาของเสี้ยน กระดูกเพิ่มขึ้นอย่างมีนัยสำคัญ ในกลุ่มฉีดยาแบบทั่วร่างกายเปรียบเทียบกับกลุ่มควบคุม ในขณะที่กลุ่มฉีดยา เฉพาะตำแหน่งส่งผลต่อคุณภาพของกระดูกในทิศทางเดียวกันกับกลุ่มฉีดยาแบบทั่วร่างกาย การฉีดยาเอเอ็มดี 3100 ลดระดับการแสดงของสารพันธุกรรม (mRNA) ของ cathepsin K, Runx2, SDF-1, RANKL และ RANKL/OPG ratio อย่างมีนัยสำคัญในกลุ่มทดลองทั้งสองกลุ่ม โดยสรุป การฉีดยาเอเอ็มดี 3100 เฉพาะ ตำแหน่ง สามารถควบคุมการเคลื่อนฟันในระยะแรก และลดกระบวนการการละลายของกระดูก ผ่านการยับยั้งกลไก SDF-1/CXCR4 axis คล้ายกับการฉีดยาแบบทั่วร่างกาย

สาขาวิชา	ทันตกรรมจัดฟัน	ลายมือชื่อนิสิต ....
ปีการศึกษา	2564	ลายมือชื่อ อ.ที่ปรึกษาหลัก ....

Narubhorn Ongprakobkul : EFFECTS OF LOCAL VERSUS SYSTEMIC ADMINISTRATION OF CXCR4 INHIBITOR AMD3100 ON ORTHODONTIC TOOTH MOVEMENT IN RATS. Advisor: Assoc. Prof. SIRIMA PETDACHAI, D.D.S., Ph.D.

Chemokines play pivotal roles in orthodontic tooth movement (OTM) through osteoclast-mediated bone resorption, but the underlying mechanism remains unclear. We aimed to elucidate the effects of serial local vs systemic administration of the chemokine receptor CXCR4 antagonist AMD3100 on OTM. The maxillary right first molar (M1) of rats was moved mesially using a 10 g of force nickel-titanium coil spring. The injections were performed every other day with phosphate-buffered saline as a control, whereas local and systemic animals were injected with AMD3100 at the buccal palatal mucosa adjacent to M1 and subcutaneously, respectively. OTM distance and alveolar bone were examined by microcomputed tomography and histologic analysis. Osteoclast numbers were quantified using TRAP staining. Cathepsin K and stromal cell-derived factor-1 (SDF-1) were evaluated using immunohistochemistry. Reverse transcriptase polymerase chain reaction for cathepsin K, Runx2, SDF-1, CXCR4, RANKL, and OPG were also examined. The results showed that OTM and osteoclast numbers were significantly decreased in the local and systemic groups compared with the control group, whereas there was no significant difference among the experimental groups. Local administration inhibited molar but not incisor movement. Trabecular thickness of the alveolar bone significantly increased in the systemic group compared with the control group, whereas local injection also affected bone quality in the same tendency as a systemic injection. AMD3100 significantly downregulated the mRNA expression levels of cathepsin K, Runx2, SDF-1, RANKL, and RANKL/OPG ratio in both experimental groups. In conclusion, local administration of AMD3100 can control initial OTM and diminish bone resorption processes during OTM via inhibition of the SDF-1/CXCR4 axis, similar to the systemic administration.

Field of Study:	Orthodontics	Student's Signature	
Academic Year:	2021	Advisor's Signature	

ACKNOWLEDGEMENTS

Narubhorn Ongprakobkul

TABLE OF CONTENTS

LIST OF FIGURES

Page

CHAPTER 1 Introduction

1.1 Background and Rationale

Orthodontic tooth movement (OTM) involves the phenomenon of immediate changes in periodontal tissue due to mechanical force application. Bone modeling and remodeling result from interactions of osteoblasts, osteoclasts, and osteocytes. In a homeostatic equilibrium, bone resorption by osteoclasts and bone formation by osteoblasts are balanced; thus, old bone is continuously replaced by new tissue that adapts to mechanical load and strain (1, 2). The compression side is characterized by cell and tissue damage, reduction in the number of patent capillaries, and partial disintegration of blood vessels, leading to ischemia and hypoxia. Conversely, periodontal ligament (PDL) reconstruction by fibroblasts and bone matrix production by osteoblast occurs on tension side (3, 4). Osteocytes that are embedded in the bone matrix extend dendrites and act as mechanoreceptors to control bone remodeling by sensing mechanical stimuli exerted by orthodontic force. These processes induce the release of chemokines and biological mediators, resulting in a specific remodeling in the PDL and alveolar bone (5). Nonetheless, the underlying mechanisms and directional specificity are still inconclusive.

Chemokines are chemotactic cytokines responsible for the establishment of chemical gradients for cell migration. Hypoxia-damaged tissue, inflammation and bone fracture can drive the upregulation of stromal cell-derived factor 1 (SDF-1), also

known as C-X-C motif chemokine 12 (CXCL12), which facilitates stem and progenitor cell retention and migration (6, 7). SDF-1 specifically binds to the chemokine receptor type 4 (CXCR4) which is a 7-transmembrane G-protein coupled receptor expressed in many cell types such as lymphocytes, bone marrow stromal cells, hematopoietic stem cells (HSCs), and cancer cells (8, 9). The bindings induce the migration of CXCR4-positive HSCs and mesenchymal stem cells (MSCs) to the repair site, initiating bone healing (7, 10). Recent studies have suggested that the SDF-1/CXCR4 axis plays a pivotal role in MSCs homing to injury sites (7, 11), early osteoclast differentiation (12, 13), bone fracture healing (6, 10, 14, 15), alveolar bone healing (16) and systemic single administration of CXCR4 antagonist AMD3100 was shown to decrease OTM with inhibition of osteoclast accumulation on the compression side of the PDL (17). Therefore, the SDF-1/CXCR4 axis may also be involved in alveolar bone remodeling at initial stage of OTM. Mobilization of stem cell from bone marrow to peripheral blood, and then to injured tissues, might reduce the SDF-1 concentration gradient (13, 18). However, previous study only emphasized on systemic single administration of CXCR4 antagonist AMD3100; thus, systemic adverse drug effects should be concerned, and the effects of local application of AMD3100 on the bone remodeling during OTM remains unclear (17).

The objective of our study aimed to elucidate the effects of serial local versus systemic administration of the CXCR4 antagonist AMD3100 on OTM and the underlying molecular mechanisms. We hypothesized that the effects of serial local

administration of AMD3100 are non-inferior to systemic administration in terms of OTM response and osteoclast accumulation via the SDF-1/CXCR4 axis. We also aimed to evaluate the changes in structural bone morphology and mRNA expression levels related to these precursors. Furthermore, we planned to explore the local effects of AMD3100 for controlling OTM in a specific location to minimize the unfavorable tooth movement and internal structure of the alveolar bone.

1.2 Research question

Is there any difference between the effects of local and systemic administration of AMD3100 on orthodontic tooth movement in rats?

1.3 Research objective

To elucidate the effects of serial local versus systemic administration of CXCR4 antagonist AMD3100 on orthodontic tooth movement (OTM) in rats.

1.4 Research hypothesis

Null hypothesis: Effects of serial local administration of AMD3100 are inferior to systemic administration on the responses of OTM and osteoclast accumulation via the SDF-1/CXCR4 axis.

Alternative hypothesis: Effects of serial local administration of AMD3100 are non-inferior to systemic administration on the responses of OTM and osteoclast accumulation via the SDF-1/CXCR4 axis.

1.5 Benefits of this study

Our study will provide clinical significance in terms of both local and systemic administrations. The anchorage control in orthodontic treatment currently utilizes a variety of sources to prevent unfavorable tooth movement such as teeth, bone, miniscrews and extraoral anchorage devices (19). However, these techniques might need patients' compliance. To avoid the drawback from traditional methods, targeted pharmacological strategies have been developed to maximize orthodontic treatment efficiency via a local application or minimally invasive technique through the cellular level regulation of osteoclastogenesis (20-23). Use of local AMD3100 to control tooth movement and increase bone thickness in specific area should be considered as a subject of interest, while treating patients receiving systemic AMD3100 as a current medication should be cautiously concerned.

1.6 Conceptual framework

(Figure 1 Conceptual framework)

CHAPTER 2 Literature review

2.1 Bone modeling, remodeling, and orthodontic tooth movement

Bone formation occurs via two pathways, known as intramembranous and endochondral ossification. Under appropriate stimuli, the bones have a potential to differentiate into a variety of tissue types. Bone modeling is an uncoupled process of activation-resorption (catabolic) or activation-formation (anabolic) on bone surfaces resulting in changes of shape, size, or position of the bone (1). Bone remodeling or turnover is a coupled local process which starts with bone resorption followed by bone formation phases. This process results in the replacement of old bone with new bone (24, 25).

Tooth movement by orthodontic force application is characterized by remodeling changes at the bone and PDL interface when an appropriate orthodontic force is applied (26). Apparently, alveolar bone resorption by osteoclasts during the OTM is an inflammatory process which occurs on trabecular and cortical bone of the compression side (27). Simultaneously, osteoblasts carry out bone formation on the tension side to maintain bone integrity during bone modeling (Fig. 2). An aseptic acute inflammatory response is occurring in the early phase of OTM, followed by an aseptic and transitory chronic inflammation. As orthodontic forces (continuous, interrupted, or intermittent) are not uniform throughout the applied region, areas of tension or compression are developed leading to varied inflammatory processes

resulting in different tissue remodeling responses (3, 4). Both bone modeling and remodeling are controlled by the cellular activities of osteoblasts, osteoclasts, and osteocytes (1, 28). These involve the removal of trenches or tunnels of bone by osteoclasts, respectively (29). Osteoblasts subsequently fill in these trenches by laying down new bone matrix. Even though bone remodeling renews the internal content of the bone without changing the size or shape of the bone under physiologic conditions, it also affects the rate of OTM (30).

The rates of bone modeling and remodeling are regulated by biochemical and mechanical factors (24, 31, 32). Activation of osteoclasts by mechanical forces, inflammatory stimuli, or hypoxia appears to be the first and necessary step in OTM. Moreover, these rates are increased by a variety of pathologic conditions affecting the skeleton including postmenopausal osteoporosis, hyperparathyroidism and rheumatoid arthritis in which local and/or systemic alterations in the levels of hormones or pro-inflammatory cytokines stimulate bone resorption (29). Most of these factors induce bone resorption predominantly by an indirect mechanism that involve upregulation of the expression of macrophage colony stimulating factor (M-CSF) and receptor activator of nuclear factor kappa-B ligand (RANKL) by osteoblasts (33).

2.2 Osteoclast–osteoblast communication

The skeletal system can function and maintain homeostasis by communication between cells from different sites such as osteoclasts and osteoblasts (34, 35). Osteoclasts are multinucleated cells originating from HSCs and share precursors with macrophages. The osteoclasts synthesize a sealed acidic compartment at the point of contact with bone, where hydrogen ions and degradative enzymes dissolve the mineral and digest the collagenous matrix. This process results in the release of calcium as well as numerous growth factors and cytokines. In contrast, cells of the osteoblast lineage such as stromal cells, bone lining cells, osteoprogenitors, preosteoblasts, osteoblasts and osteocytes are derived from MSCs within the bone marrow stroma, which also can differentiate into fibroblasts, chondrocytes, myoblasts and adipocytes under the appropriate stimuli. These cells synthesize an extracellular matrix (ECM), made mostly of type I collagen and several non-collagenous proteins. Osteoclast–osteoblast interactions occur at various stages of differentiation.

2.3 Biological mediators during OTM

To the best of our knowledge, the production of biological mediators from the PDL cells plays a vital role in activating tissue remodeling (36). Several theoretical processes have been presented in literature to clarify the basic mechanism of OTM (3, 37). When the tooth is subjected to orthodontic force, the blood vessel system in PDL is gradually occluded, resulting in circulatory disturbances and leading to ischemia and local hypoxia on the compression side. PDL cells elicit osteoclast formation through regulating the expression of related agents, including RANKL and osteoprotegerin (OPG). Low oxygen level has been reported to activate hypoxia inducible factor 1α (HIF-1α) and regulate bone resorption through enhancement of osteoclast differentiation and activity (38). Recently, HIF-1α was found to up-regulate RANKL expression in PDL cells (39). These findings illustrate that oxygen tension might be involved in osteoclastogenesis during OTM (40). Mediators such as cytokines, growth factors and hormones seem to mediate the conversion of mechanical force into a biological response. Signals generated by mechanical stimulation are transmitted between cells and extracellular matrix through gap junction channels causing cell activation and differentiation. Understanding of molecular mechanisms that regulate the activation of osteoclasts precursors in the PDL has advanced rapidly following the identification in the mid-to-late 1990s.

RANKL/RANK/OPG system is essential in osteoclastogenesis and bone resorption. RANKL, a 317 amino acid peptide transmembrane glycoprotein, is a member of the tumor necrosis factor (TNF) superfamily. RANKL interacts with its receptor on osteoclast precursors called receptor activator of nuclear factor kappa-B (RANK). The RANKL/RANK interaction results in activation, differentiation, and fusion of hematopoietic cells of the osteoclast lineage leading to the process of bone resorption. Interaction between RANK-expressing osteoclast precursors and RANKL-expressing osteoblasts is essential for osteoclastogenesis. RANK signaling activates an osteoclastogenic cascade of transcription factors such as NF-κB, AP-1 (c-Fos) and NFATc1. Several soluble factors enhance osteoclastogenesis through RANKL induction in osteoblasts including parathyroid hormone (PTH), parathyroid hormone-related peptide (PTHrP), TNF-α, thyroid hormone, interleukin-1 (IL-1), interleukin-11 (IL-11), 1,25-$(OH)_2$ vitamin D_3 and prostaglandin E_2 (PGE_2). Most modulate the cyclic AMP/protein kinase A (PKA) pathway. The expression of OPG simultaneously upregulated at the tension side (41-43). OPG inhibits RANKL/RANK interaction by acting as a decoy receptor (a soluble receptor acting as antagonist) for RANKL which inhibits RANK signaling by masking RANKL. Several studies revealed that in-vitro compressive forces increased the expression of RANKL and decreased the expression of OPG in osteoblasts and PDL cells (44). OPG interferes with osteoclast–osteoblast

interactions, and the RANKL/OPG ratio is indicator of osteoclastogenic activity in various bone remodeling diseases.

Critical factors of osteoclastogenesis and transcription factors such as runt-related transcription factor 2 (Runx2), cathepsin K, cytokines, PGs, TNFs, and proteases are also expressed in PDL during in-vivo OTM (5, 45). These markers are related with the remodeling of PDL and bone. Runx2 functions promote the osteogenic differentiation of progenitor cells and pre-osteoblast, literally found increasing during tooth movement (46). Moreover, the degradation of extracellular matrix also depends on the production of cathepsins and MMP's proteases which produced by fibroblasts and osteoblasts. These markers stimulate ECM degradation through autocrine and paracrine actions (5, 47).

2.4 SDF-1/CXCR4 axis

Chemokines are the vital regulators of cell communication and adhesion which target specifically to G-protein-coupled seven-span transmembrane receptors. Cell migration, recruitment, and homing to the injure site are important for the healing process and bone remodeling. Hypoxia at the damage site and the expression of transcription factor HIF-1α were found to drive the upregulation of SDF-1 production resulting in the increase of adhesion, migration and homing of circulating CXCR4-positive progenitor cells to ischemic tissue (6, 7, 49).

The ligand for CXCR4, SDF-1, is a well-known chemokine that plays a crucial role in trafficking of HSCs activation, mobilization, homing and retention. SDF-1 has been reported to be expressed by stromal and endothelial cells, including bone marrow, heart, skeletal muscle, liver, brain and kidney. During injury, stem cells are recruited from the bone marrow and navigated to the site of injury by SDF-1 chemotactic responses. This phenomenon causes changes in cell adhesion and cell secretion, turning to guide HSCs to migrate across the basal lamina of the endothelium toward a high concentration gradient of SDF-1. HSCs are navigated to the site of injury and remain there long enough to participate in tissue repair (9). SDF-1 secretion increases in these organs during tissue damage such as heart infarct, limb ischemia, toxic liver damage, excessive bleeding, total body irradiation and after tissue damage related to chemotherapy. Molecular-leveled studies show that the

SDF-1 expression is upregulated in endothelial cells by HIF-1α, since the SDF-1 promoter, as the CXCR4 promoter, contains HIF-1α binding sites (49). Thus, HIF-1α elevates the SDF-1 expression in hypoxic and damaged tissues, which leads to the chemoattraction of CXCR4 participating in regenerative process. In conclusion, SDF-1 appears to be a pivotal indicator for hypoxic tissue-organ injuries and involved in the active recruitment of HSCs for repair of damaged tissue, implicating this chemokine as an important maintenance factor in tissue repair.

CXCR4 is a 7-transmembrane G-protein coupled receptor which function as a receptor for SDF-1. CXCR4 is regulated at several levels including the transcriptional level by hypoxic condition. HIF-1α in cooperation with nuclear factor-κB (NF-κB) was found to upregulate expression of CXCR4-positive HSCs and MSCs (48). CXCR4 binding with SDF-1 undergoes dimerization, and the activated SDF-1–CXCR4 complex is rapidly internalized from cell surface in a mechanism involving G-protein-coupled receptor kinases. This axis plays an important role in hematopoiesis, vascular development, immune regulation, inflammatory diseases and bone remodeling. Recent studies revealed that the SDF-1/CXCR4 axis involved in alveolar bone healing and bone fracture healing (6, 50). Moreover, this axis activates several signaling pathways in target cells which crucial for both trafficking and interaction with the intercellular environment (Fig. 3).

2.5 AMD3100: Therapeutic modulation of the SDF-1/CXCR4 axis

As the SDF-1/CXCR4 axis has emerged as an important regulator of trafficking of normal stem cells and metastasis of carcinoma stem cells, it became a molecular target for various therapeutic interventions (Fig. 4). In several studies, AMD3100, also known as plerixafor and Mozobil®, was reported as a selective antagonist of the CXCR4 which rapidly mobilizes stem and progenitor cells in bone marrow niche to the peripheral circulation. Blockage of CXCR4 receptor by AMD3100 is currently successfully employed to mobilize HSCs from bone marrow into peripheral blood. Small molecular inhibitors of CXCR4 had been reported to inhibit growth and metastasis of experimental tumors in animal models. The mechanism of action of AMD3100 is high-affinity competitive blocking of CXCR4 receptor and disrupting their attraction to SDF-1 (51). AMD3100 is currently used to mobilized HSCs for bone marrow transplantation (52, 53) multiple myeloma and Non-Hodgkin's Lymphoma (54). Nevertheless, AMD3100 is quickly absorbed and reach highest concentration at 30 to 60 minutes after the administration. It also has short plasma half-life, only 3 to 5 hours, and 70% of drug excreted via kidneys within 24 hours (53).

In conclusion, the SDF-1/CXCR4 axis plays an important role in several processes related to development, regeneration of normal stem cells and progression of malignancies. The explanation is that both normal and malignant stem cells express functional CXCR4. Thus, several strategies aimed at inhibiting the SDF-1/CXCR4 axis to find practical application in the clinical practice.

CHAPTER 3 Research methodology

3.1 Experimental animals

Eighteen six-week-old male Wistar/ST rats (Sankyo-lab, Tokyo, Japan) were randomly divided into three groups with six rats in each group, consisting of control with OTM, local and systemic administrations of SDF-1 antagonist, AMD3100 with OTM. All rats were acclimatized for one week, fed with powdered diet (RI-Sterile feed CE-2 powder type, CLEA Japan, Tokyo, Japan), given water ad libitum, and housed under a controlled environment (22 ± 1 °C, standard 12-h light-dark cycle) throughout the experimental period.

3.2 Ethical consideration

All animal experiments have been approved by the Institutional Animal Care and Use Committee of Tokyo Medical and Dental University (A2018-119C3, A2019-341A).

3.3 Materials

- Mixed anesthetic (medetomidine, 0.3 mg/kg; midazolam, 4 mg/kg; butorphanol, 5 mg/kg) and Antisedan (atipamezole, 0.75mg/kg)

- Powder diet (RI-Sterile feed CE-2 powder type, CLEA Japan, Tokyo, Japan)

- Nickel-titanium closing coil spring (Tomy international, Tokyo, Japan)

- Ligature wire (Tomy international)

- Light-curing composite resin (GC, Tokyo, Japan)

- Phosphate-buffered saline (PBS) (pH 7.4, FUJIFILM Wako Pure Chemicals)

- AMD3100 (AdooQ Bioscience, CA, USA)

- Paraformaldehyde (4%, pH 7.4, FUJIFILM Wako Pure Chemicals, Osaka, Japan)

- 2% Isoflurane inhalant

- Cryofilm tranfer kit (Finetec, Tokyo, Japan)

- 5% super cryoembedding medium (SCEM) gel (Leica Biosystems, Nussloch, Germany)

- TRAP/ALP double-staining kit (Code 294–67001, FUJIFILM Wako Pure Chemical)

- Hematoxylin and eosin (Wako Pure Chemicals)

- Avidin-biotin complex (VECTASTAIN® ABC Kit Rabbit IgG; Vector Laboratories, Burlingame, CA, USA)

- Diaminobenzidine substrate (ImmPACT™ DAB, SK-4105, Vector Laboratories)

- Rabbit anti-cathepsin K antibody (1:100, ab19027, Abcam, Cambridge, UK)

- Rabbit anti-SDF1 antibody (1:100, bs-4938R, Bioss Antibodies, MA, USA)

- PureLink FFPE Total RNA Isolation Kit (Invitrogen, Carlsbad, CA, USA)

- PrimeScript RT Master Mix (Perfect Real Time) Kit (Takara Bio, Shiga, Japan)

- TaqMan® Gene Expression Assays (Takara Bio)

- Primers for real-time PCR amplification of genes encoding are as follows:

  cathepsin K (NM_031560.2), Runx2 (NM_001278483.1), SDF-1

  (NM_022177.3), CXCR4 (NM_022205.3), RANKL (NM_057149.1), OPG

  (NM_012870.2) and GAPDH (NM_017008)

3.4 Equipments

- Micro-computed tomography (micro-CT) (R_mCT2; Rigaku, Tokyo, Japan)

- Desktop X-ray micro-CT system (SMX-100CT; Shimadzu, Kyoto, Japan)

- Three-dimensional (3D) image-analysis software (TRI/3-D-BON; RATOC
  System Engineering Co., Tokyo, Japan)

- CM3050s cryostat machine (Leica Biosystems)

- Image J software (National Institutes of Health, Bethesda, MD, USA)

- Confocal microscope (NIKON ECLIPSE 80i, Nikon, Tokyo, Japan)

- Laser capture microdissection (LMD7000; LEICA Biosystems)

- 7500 Real-Time PCR System (Applied Biosystems; Thermo Fisher Scientific,
  CA, USA)

- Needle 34G (Pasny; Nanbu, Tokyo, Japan)

- Syringe lock type 1 ml (Nanbu, Tokyo, Japan)

- Carbon dioxide gas equipment

3.5 Research methods

3.5.1 Research plan

(Figure 5 Diagram of research methods)

3.5.2 Experimental design

(1) Orthodontic tooth movement (OTM) model

The experimental procedures were established based on the previous study (23, 55). Animals were placed under general anesthesia with medetomidine (0.3 mg/kg), midazolam (4 mg/kg), and butorphanol (5 mg/kg). The upper right first molar (M1) of the rats was moved mesially using a 10-g force nickel-titanium closed coil spring (Tomy international, Tokyo, Japan) attached to the upper incisor, tied with a ligature wire (Tomy international), and fixed with a light-curing composite resin (GC, Tokyo, Japan) (Fig. 6). After placement of the coil spring, the animals of the control group were treated with phosphate-buffered saline (PBS), while the animals in the local group were injected with AMD3100 (AdooQ Bioscience, CA, USA) at buccal and palatal mucosa adjacent to M1 (1000 μM; 0.25 mg/kg) (20, 23, 56) and subcutaneously (1000 μM; 5 mg/kg) in the systemic group (17), respectively. The injections were performed every other day: at 0, 2, 4, 6, 8, 10 and 12 days under general anesthesia, until the end of the experiment. Meanwhile, the appliances were checked at the same time as the injections. When the appliances broken or loosened, a new coil spring was placed under the anesthesia with the same manner.

Furthermore, the incisors malocclusion was checked simultaneously. The incisor trimming would be provided in case of the incisors either contacting with the buccal soft tissue or protruding outwardly, to prevent the risk of trauma or accident.

(2) Micro-computed tomography (micro-CT) analysis

After general inhalation anesthesia with 2% Isoflurane inhalant, the animal body was placed in prone position. The head was scanned by micro-computed tomography (micro-CT) (R_mCT2; Rigaku, Tokyo, Japan) at 0, 1, 3, 7 and 14 days after starting OTM with the conditions of 90 kV, 160 mA and 30-mm field of view (FOV). The distance from the distal surface of maxillary M1 to the mesial surface of the maxillary second molar (M2) was measured from micro-CT images as the OTM distance. We also determined the distant effects of AMD3100 through analysis of the incisor retraction between the labial surface of maxillary incisor at the gingival margin to the distal surface of maxillary third molar (M3) and calculated the orthodontic anchorage expressed as the ratio of incisor to molar tooth movement (21, 23).

Animals were sacrificed by carbon dioxide gas at 14 days after starting OTM. The maxillae were resected immediately and scanned using a desktop X-ray micro-CT system (SMX-100CT; Shimadzu, Kyoto, Japan) with a scanning resolution of 20-μm intervals on individual images. The interradicular alveolar bone in the maxillary M1 was chosen as the region of interest (ROI) for bone analysis (Fig. 7). Changes of structural morphology in the ROI were analyzed in the aspect of trabecular thickness

(Tb.Th), trabecular number (Tb.N), trabecular separation (Tb.Sp), trabecular spacing (Tb.Spac), total callus volume (TV), mineralized bone volume (BV), and bone volume fraction (BV/TV) using three-dimensional (3D) image analysis software (TRI/3-D-BON; RATOC System Engineering Co., Tokyo, Japan) according to the instructions of the manufacturer (57).

(3) Preparation of histological sections

After the sacrifice, the maxillae were resected immediately and fixed with paraformaldehyde (4%, pH 7.4, FUJIFILM Wako Pure Chemicals, Osaka, Japan) at room temperature for 24 hours, and then stored in phosphate-buffered saline (PBS) (pH 7.4, FUJIFILM Wako Pure Chemicals) at 4 ℃.

Frozen non-decalcified sections were prepared with a cryofilm tranfer kit (Finetec, Tokyo, Japan) (58). The isolated right hemimaxillae were snapped freezing by immersion in cold liquid hexane, then embedded in 5% super cryoembedding medium (SCEM) gel (Leica Biosystems, Nussloch, Germany) and quenched with cold liquid hexane until completely frozen. The frozen super cryoembedding medium (SCEM) blocks were cut into horizontal serial sections at a thickness of 10 μm with a disposable carbide tungsten steel blade using a CM3050s cryostat machine (Leica Biosystems). Some frozen sections were stained with hematoxylin and eosin (HE) for schematic representation and further histological observations.

(4) Tartrate resistant acid phosphatase (TRAP) staining

TRAP expression was assessed by staining with the TRAP/ALP double-staining kit (Code 294–67001, FUJIFILM Wako Pure Chemical) to evaluate osteoclast accumulation. Following the manufacturer's protocol, sections were incubated in TRAP buffer for 30 min and then washed with distilled water 3 times. Osteoclasts were stained red with TRAP staining solution, while nuclei were counterstained with hematoxylin solution. These sections were used to count the number of TRAP-positive multinucleated cells in the PDL on the compression side of the mesial root of M1 by a single examiner on three randomized sections from each sample, and the averages were calculated for each group. The circumferential length of the alveolar bone surface along the compression side of the mesial root was measured five times using Image J software (National Institutes of Health, Bethesda, MD, USA) to determine the average. The results were expressed as mean ± standard deviation of the number of multinucleated TRAP-positive cells per mm of the alveolar bone surface.

(5) Immunohistochemical analysis

Frozen horizontal sections of mesial roots of M1 at the level less than 180 μm from the furcation region were determined for the detection of cathepsin K and SDF-1 expressions in the PDL by the avidin-biotin complex (VECTASTAIN® ABC Kit Rabbit IgG; Vector Laboratories, Burlingame, CA, USA) according to the manufacturer's

instructions. Briefly, sections from each group were subsequently subjected to antigen retrieval, blocked with blocking solution (BLOXALL™; SP-6000, Vector Laboratories) to prevent endogenous peroxidase activity for 10 min, and incubated with normal blocking serum (VECTASTAIN® Elite ABC kit, Vector Laboratories) for 20 min at 37 °C. After blotting excess serum, sections were incubated with either rabbit anti-cathepsin K antibody (1:100, ab19027, Abcam, Cambridge, UK) or rabbit anti-SDF1 antibody (1:100, bs-4938R; Bioss Antibodies, MA, USA) overnight in a humidified chamber at 4 °C. Biotinylated secondary antibodies against the primary antibodies were applied, followed by avidin-biotin complex (VECTASTAIN® Elite ABC kit, Vector Laboratories). Consequently, sites of peroxidase activity were visualized with diaminobenzidine substrate (ImmPACT™ DAB, SK-4105, Vector Laboratories), and the sections were counterstained with hematoxylin (Fig. 8). Images of immunostaining sections were observed under a confocal microscope (NIKON ECLIPSE 80i, Nikon, Tokyo, Japan).

(6) Quantitative real-time polymerase chain reaction (qRT-PCR) analysis

After histological observations, periapical PDL tissue was collected from the compression side of the mesial roots of the maxillary M1 using laser capture microdissection (LMD7000; LEICA Biosystems) (Fig. 9). Total RNA was extracted using a PureLink FFPE Total RNA Isolation Kit (Invitrogen, Carlsbad, CA, USA). Isolated total RNA was converted into complementary DNA via reverse transcription with random

primers using the PrimeScript RT Master Mix (Perfect Real Time) Kit (Takara Bio, Shiga, Japan). Real-time PCR assays were quantified in triplicate for each sample by a 7500 Real-Time PCR System (Applied Biosystems; Thermo Fisher Scientific, CA, USA) using gene-specific primers (Takara Bio) and TaqMan® Gene Expression Assays (Applied Biosystems). The appropriate primers that were chosen for real-time PCR amplification of genes encoding are as follows: *cathepsin K* (NM_031560.2), *Runx2* (NM_001278483.1), *SDF-1* (NM_022177.3), *CXCR4* (NM_022205.3), *RANKL* (NM_057149.1), *OPG* (NM_012870.2) and *GAPDH* (NM_017008). Gene expression levels were calculated according to the comparative Ct method of relative quantification, and GAPDH was used as the housekeeping gene for normalization.

3.6 Statistical analysis

All statistical analyses were performed using statistical software (IBM SPSS Statistics Version 22.0; SPSS Statistics, Inc., Armonk, NY, USA). Results are presented as the mean ± standard deviation. After testing for normality and equality in variances, intergroup comparisons were conducted via one-way analysis of variance followed by Tukey's post-hoc test. Data with a *p* value less than 0.05 ($P < 0.05$) were considered statistically significant.

CHAPTER 4 Results

4.1 Animals' body weights

The animals' body weights were observed every other day. The findings showed increased body weight in a normal pattern throughout the experimental period. There was no significant difference at any stage among groups until the end of the experiment (data not shown).

4.2 Orthodontic tooth movement (OTM) distance

Micro-CT analysis showed that the amount of OTM distance significantly decreased in the local and systemic groups compared with the control group in every observed period: days 1, 3, 7, and 14 (P <0.05). Conversely, there was no significant difference in the molar movement between local and systemic administration throughout the experimental period. On day 14, molars with PBS injection (control group) moved 0.45 ± 0.10 mm. The mean distance of molar movement in the local and systemic injection of AMD3100 groups was 0.33 ± 0.03 mm (26% reduction relative to the control group, P <0.05) and 0.30 ± 0.07 mm (35% reduction relative to the control group, P <0.05), respectively (Fig 10, A).

The amount of incisal retraction was also measured to determine whether the local injections spread particularly adjacent to M1 without distant effects on incisal tooth movement. There was no significant difference in incisor retraction between the control and local injection groups. In contrast, the incisor retraction was

significantly reduced in animals receiving a systemic injection of AMD3100 compared with the other groups (68% and 60% less than in the control and local groups, respectively) (P <0.05) (Figs 10, B and C).

4.3 Alveolar bone analysis

For the alveolar bone analysis on day 14, trabecular thickness (Tb.Th) and trabecular spacing (Tb.Spac) significantly increased (P <0.05), whereas trabecular number (Tb.N) significantly decreased (P <0.05) in the systemic group compared with the control group. The local injection affected bone quality similarly to a systemic injection without a significant difference between the local and systemic groups (Figs 11, A, B, and D).

TV, mineralized BV, and bone volume fraction (BV/TV) subsequently decreased in control, local, and systemic groups (Figs 11, E-G). In contrast, the highest trabecular separation (Tb.Sp) was found in the systemic group, followed by the local and control groups (Fig. 11, C). However, the differences in these parameters among the groups were not significant.

4.4 Histological observation

The mesial root of the maxillary M1 was stained with HE for schematic observation. We found narrowing of the PDL space and Howship's lacunae along the compression side without inflammation in every group from the HE stained sections.

The widening of the PDL space and stretched collagen fibers were observed on the

tension side. We also found blood vessels and bone finger projections (Fig. 12).

4.5 Tartrate resistant acid phosphatase (TRAP) staining

We quantified osteoclast accumulation on the compression side of the PDL

using TRAP staining and compared the amount of TRAP-positive multinucleated

osteoclasts along the compression side of the PDL among the 3 groups. In the

control group, osteoclast cells were abundantly found on the mesial side of the

alveolar bone (15.75 ± 3.89 cells/section). The data demonstrated a significant

reduction in the number of osteoclast cells in the local group (4.04 ± 1.83

cells/section; P <0.05) as well as in the systemic group (6.22 ± 1.55 cells/section; P

<0.05) compared with the control group. Moreover, there was no significant

difference in the number of osteoclast cells between the local and systemic groups

(Fig 13).

4.6 Immunohistochemical analysis

The expressions of cathepsin K (Figs 14, A-C) and SDF-1 (Figs 14, D-F) were

detected by ABC immunostaining and visualized by the DAB substrate. We observed

a dark brown color on the mesial root of M1, which represented a positive result. On

the compression side, the extracellular matrix of the PDL cells showed a positive

dark brown color only in the control group for both anti-cathepsin K and anti-SDF1

targets (Figs 14, A and D). The anti-cathepsin K target became slightly light brown in

the PDL cells of the systemic group (Fig 14, C), and the color remained unchanged in the local group (Fig 14, B). For anti-SDF-1, the color turned slightly light brown for both the local and systemic groups (Fig 14, E and F).

4.7 Quantitative real-time polymerase chain reaction (qRT-PCR) analysis

Orthodontic force combined with either local or systemic AMD3100 administration significantly downregulated the mRNA expression levels of cathepsin K, Runx2, SDF-1, RANKL, and RANKL/OPG ratio in the PDL on the compression side without significant difference between the local and systemic groups. When compared with the control group, a 5.4-fold and 4.3-fold reduction in cathepsin K expression were detected in the local and systemic groups, respectively (Fig 15, A). Runx2 mRNA level also showed a 3.1-fold decrease in a local and 6.4-fold decrease in the systemic group compared with the control group (Fig 15, B).

Real-time PCR showed that SDF-1 mRNA levels significantly decreased in the systemic injection (P <0.05), whereas the local injection group had a tendency similar to that of the systemic group when compared with the control animals (Fig 15, C). CXCR4 expression also decreased in the local and systemic groups; however, there was no significant difference among groups (Fig 15, D).

Moreover, the mRNA levels of RANKL, OPG, and RANKL/OPG ratio were analyzed to observe osteoclast-osteoblast differentiation. RANKL expression levels were 7.92-fold and 8.11-fold significantly decreased in the local and systemic groups

compared with the control group (Fig 15, E). Conversely, OPG mRNA levels tended to be higher in the systemic group than in the local and control groups (Fig 15, F). Consequently, the RANKL/OPG ratio was significantly decreased in the local and systemic groups compared with the control group (P <0.05) (Fig 15, G).

CHAPTER 5 Discussion

Cell migration, recruitment, and homing to the injury site are important for initiating the healing process and bone remodeling. Hypoxia at the damage site and the expression of transcription factor hypoxia-inducible factor-1 a-subunit may drive the upregulation of SDF-1 production, increasing adhesion, migration, and homing of circulating CXCR4-positive progenitor cells, such as HSCs, to the ischemic tissue (6, 7, 49). As the orthodontic force is applied to the teeth, inflammation and regional hypoxia occur on the compression side of the PDL after tooth movement similar to the wound site (3, 4, 11), and the expression of SDF-1 in the PDL has also been reported in previous studies (50). Taken together, it can be considered that SDF-1 production plays a crucial role in the accumulation of HSCs and increases the number of TRAP-positive multinuclear osteoclasts on the compression side of the PDL.

In several studies, AMD3100 was reported as a selective antagonist of CXCR4, which rapidly mobilizes stem and progenitor cells from the bone marrow niche to the peripheral circulation (6, 7, 11). The mechanism of action of AMD3100 is high-affinity competitive blocking of the CXCR4 receptor and disrupting their attraction to SDF-1 (51). AMD3100 is currently used to mobilize HSCs for bone marrow transplantation (52, 53) multiple myeloma and non-Hodgkin's lymphoma (54). Nevertheless, AMD3100 is quickly absorbed and reaches the highest concentration at

30-60 minutes after administration. It also has a short plasma half-life, only 3-5 hours, and 70% of the drug is excreted via the kidneys within 24 hours (53). Therefore, AMD3100 was continuously administrated during the experimental period to explore the role of the SDF-1/CXCR4 axis in the OTM process and alveolar bone response.

Setting the proper ROI for bone analysis in the OTM model is difficult. Machado et al (59) demonstrated that alveolar bone remodeling under OTM varies according to the height of the ROI, even in the alveolar bone mesial to the mesial root of rats. For instance, bone resorption occurs near the cervical area, whereas bone apposition occurs near the root apex in the alveolar bone surrounding the mesial root of the maxillary first molar of the rat during OTM. In addition, the width of the alveolar bone mesial to the mesial root is narrow enough to set an ROI of sufficient size because of the maxillary sinus space and the height of the alveolar bone mesial to the mesial root was very unstable after OTM. Therefore, we set the ROI for the bone analysis in the interradicular septal bone area as we performed. Indeed, the same/similar ROI was commonly set for micro-CT analysis in the literature (20, 60, 61).

In this study, to examine the effectiveness of local vs systemic inhibition of the SDF-1/CXCR4 axis in OTM, we administered serial local and systemic injections of AMD3100 to inhibit signaling while applying the orthodontic force to the maxillary M1. The experimental procedures were designed for 14 days as previously reported to reach the phase of tooth movement in a rodent model (62). The results

demonstrated that serial local injection of AMD3100 could decrease the amount of OTM and multinucleated osteoclast accumulation on the compression side of the PDL in the same manner as the systemic injection. Importantly, local administration of AMD3100 did not inhibit incisor retraction, whereas systemic administration hindered incisor retraction. These results indicate that the local injection of AMD3100 affected the areas adjacent to the injection site and particularly spread only on M1 without distant tooth movement effects. It is noted that the decrease in OTM in local and systemic administration conformed to the significantly reduced number of TRAP-positive multinucleated osteoclasts and corresponded with the expression of cathepsin K in the immunohistochemical analysis.

Our study also revealed that SDF-1/CXCR4 blockade results in a significant increase in Tb.Th, Tb.Spac, and decrease of Tb.N in the serial AMD3100-treated group. Both experimental groups showed increased trabecular thickness, implying that the individual strut was thicker from a more rapid developmental stage of endochondral ossification (52). Moreover, histomorphometric analysis of the callus showed a decreasing tendency in TV, BV, and BV/TV with AMD3100 injections. Other studies related to long-term administration of AMD3100 also reported similar results throughout fracture healing using only AMD3100 (6, 63) and changed the bone structures in a distraction osteogenesis model (56). From our previous study, we demonstrated the relationship between OTM and the SDF-1/CXCR4 axis by administering a systemic single injection of AMD3100 (17). The results showed

delayed OTM in rat molars on the first day under orthodontic force application. There was no significant difference in alveolar bone structural evaluation, but systemic adverse drug effects should be considered (17). In conclusion, our findings suggest that serial injections of AMD3100 have the potential to enhance the bone healing process during orthodontic treatment.

Herein, we demonstrated that inhibition of SDF-1/CXCR4 signaling during tooth movement with AMD3100 treatment leads to a significantly decreased gene expression of cathepsin K, Runx2, and RANKL are the indicators of osteoclastogenesis and osteogenic differentiation (12, 47, 56, 64). Cathepsin K expression was related to the osteoclastogenesis and degradation of the extracellular matrix in the PDL (5). Moreover, Runx2 expression was found to be one of the critical factors in osteogenic differentiation of progenitor cells and preosteoblasts, which were found to increase during tooth movement (46). A recent study in MSCs revealed that blocking the SDF-1/CXCR4 axis inhibited Runx2 expression (12). During OTM, the RANKL/RANK/OPG system is essential in osteoclastogenesis and bone resorption. Several studies have revealed that in vitro compressive forces increase the expression of RANKL and decrease the expression of OPG in PDL cells (3, 5). OPG interferes with osteoclast-osteoblast interactions, and the RANKL/OPG ratio indicates osteoclastogenic activity in various bone remodeling diseases.

Furthermore, SDF-1 and CXCR4 gene expression were also reduced by the serial administration of AMD3100. This phenomenon could involve a biphasic

mobilization pattern, which depends on the SDF-1 niche. According to a previous study, continuous injection of AMD3100 induced a rapid displacement and release of SDF-1, which peaked at 6 hours, then rapidly declined within the first 24 hours and below the baseline after 72 hours of treatment compared with the PBS-treated control (65). Our findings were similar to those of previous studies, and it is worth noting that there was no significant difference between local and systemic administration.

The anchorage control in orthodontics treatment currently uses a variety of sources to prevent unfavorable tooth movements, such as teeth, elastics, maxillofacial functions, and extraoral anchorage devices (19). However, these techniques might need patient compliance. To avoid the drawbacks of traditional methods, targeted pharmacologic strategies have been developed to maximize orthodontic treatment efficiency via a local application or minimally invasive technique through the cellular level regulation of osteoclastogenesis (20-23). Our study clearly showed the local administration of an SDF-1 blocker, AMD3100, as a patients' dependent pharmacologic approach to reinforce the anchorage in the initial stage of OTM. These techniques might be useful in several situations. For instance, the inhibition of bone resorption is desirable at specific locations in the case of enhancing orthodontic anchorage or treatment of localized osteolytic diseases.

This study has several limitations. First, the detailed molecular mechanisms determining the degree of local and systemic administration spreading remain

unclear because of the pharmacokinetics of AMD3100. The volume of distribution, clearance rate, and elimination half-life were very short, leading to difficulty detecting the amount of AMD3100 in serum. Second, the long-term model was not examined in this study; therefore, it remains unclear whether the SDF-1/CXCR4 axis plays a crucial role in the late stage of OTM. An earlier time point study for alveolar bone analysis and osteoclast quantification to monitor changes in the initial drug delivery should be examined to further investigate the pragmatic approach of pharmacologic anchorage control.

In summary, OTM promotes an increase in SDF-1 expression. Local application of the SDF-1/CXCR4 signaling antagonist AMD3100 may significantly hinder bone mineralization and osteogenic differentiation. This finding may suggest novel therapeutic manipulation of osteoprogenitor cell homing and differentiation in patients undergoing orthodontic treatment. Despite using fewer doses of AMD3100, serial local administration of AMD3100 inhibited OTM. It also affected bone properties and osteoclast accumulation, similar to systemic administration. These findings revealed that local administration of AMD3100 was effective in alveolar bone metabolism during OTM via inhibition of the SDF-1/CXCR4 axis with less systemic side effects and higher cost-effectiveness than systemic administration. Thus, our study promoted clinical significance in both local and systemic administrations. The use of local AMD3100 to increase bone thickness in specific areas should be considered a

subject of interest while treating patients receiving systemic AMD3100 as a current medication should be cautiously considered.

CHAPTER 6 Conclusion

Serial local administration of AMD3100 decreased OTM and osteoclast accumulation via the SDF-1/CXCR4 axis, which was noninferior to systemic administration. Moreover, serial local and systemic administration of AMD3100 could alter the structural bone morphology and mRNA expression levels. Interestingly, we also found that serial local administration could control initial OTM by inhibiting molar movement but not incisor retraction. In addition, our study enlightened about local administration of AMD3100 as the novel therapeutic approach which has comparable treatment outcomes to systemic administration with lower adverse effects.

REFERENCES

1.	Frost HM. Skeletal structural adaptations to mechanical usage (SATMU): 2. Redefining Wolff's law: the remodeling problem. Anat Rec. 1990;226(4):414-22.

2.	Nakahama K. Cellular communications in bone homeostasis and repair. Cell Mol Life Sci. 2010;67(23):4001-9.

3.	Krishnan V, Davidovitch Z. Cellular, molecular, and tissue-level reactions to orthodontic force. Am J Orthod Dentofacial Orthop. 2006;129(4):469 e1-32.

4.	Meikle MC. The tissue, cellular, and molecular regulation of orthodontic tooth movement: 100 years after Carl Sandstedt. Eur J Orthod. 2006;28(3):221-40.

5.	Vansant L, Cadenas De Llano-Perula M, Verdonck A, Willems G. Expression of biological mediators during orthodontic tooth movement: A systematic review. Arch Oral Biol. 2018;95:170-86.

6.	Toupadakis CA, Wong A, Genetos DC, Chung DJ, Murugesh D, Anderson MJ, et al. Long-term administration of AMD3100, an antagonist of SDF-1/CXCR4 signaling, alters fracture repair. J Orthop Res. 2012;30(11):1853-9.

7.	Yellowley C. CXCL12/CXCR4 signaling and other recruitment and homing pathways in fracture repair. Bonekey Rep. 2013;2:300.

8.	Jung Y, Wang J, Schneider A, Sun YX, Koh-Paige AJ, Osman NI, et al. Regulation of SDF-1 (CXCL12) production by osteoblasts; a possible mechanism for stem cell homing. Bone. 2006;38(4):497-508.

9.	Lau TT, Wang D-A. Stromal cell-derived factor-1 (SDF-1): homing factor for engineered regenerative medicine. Expert Opinion on Biological Therapy. 2011;11(2):189-97.

10.	Ho CY, Sanghani A, Hua J, Coathup M, Kalia P, Blunn G. Mesenchymal stem cells with increased stromal cell-derived factor 1 expression enhanced fracture healing. Tissue Eng Part A. 2015;21(3-4):594-602.

11.	Hocking AM. The Role of Chemokines in Mesenchymal Stem Cell Homing to Wounds. Adv Wound Care (New Rochelle). 2015;4(11):623-30.

12.	Hosogane N, Huang Z, Rawlins BA, Liu X, Boachie-Adjei O, Boskey AL, et al.

Stromal derived factor-1 regulates bone morphogenetic protein 2-induced osteogenic differentiation of primary mesenchymal stem cells. Int J Biochem Cell Biol. 2010;42(7):1132-41.

13.   Wright LM, Maloney W, Yu X, Kindle L, Collin-Osdoby P, Osdoby P. Stromal cell-derived factor-1 binding to its chemokine receptor CXCR4 on precursor cells promotes the chemotactic recruitment, development and survival of human osteoclasts. Bone. 2005;36(5):840-53.

14.   Kitaori T, Ito H, Schwarz EM, Tsutsumi R, Yoshitomi H, Oishi S, et al. Stromal cell-derived factor 1/CXCR4 signaling is critical for the recruitment of mesenchymal stem cells to the fracture site during skeletal repair in a mouse model. Arthritis Rheum. 2009;60(3):813-23.

15.   Okada K, Kawao N, Yano M, Tamura Y, Kurashimo S, Okumoto K, et al. Stromal cell-derived factor-1 mediates changes of bone marrow stem cells during the bone repair process. Am J Physiol Endocrinol Metab. 2016;310(1):E15-23.

16.   Kimura Y, Komaki M, Iwasaki K, Sata M, Izumi Y, Morita I. Recruitment of bone marrow-derived cells to periodontal tissue defects. Front Cell Dev Biol. 2014;2:19.

17.   Hatano K, Ishida Y, Yamaguchi H, Hosomichi J, Suzuki JI, Usumi-Fujita R, et al. The chemokine receptor type 4 antagonist, AMD3100, interrupts experimental tooth movement in rats. Arch Oral Biol. 2018;86:35-9.

18.   Guo Y, Hangoc G, Bian H, Pelus LM, Broxmeyer HE. SDF-1/CXCL12 enhances survival and chemotaxis of murine embryonic stem cells and production of primitive and definitive hematopoietic progenitor cells. Stem Cells. 2005;23(9):1324-32.

19.   Costa A, Raffainl M, Melsen B. Miniscrews as orthodontic anchorage: a preliminary report. Int J Adult Orthodon Orthognath Surg. 1998;13(3):201-9.

20.   Chang JH, Chen PJ, Arul MR, Dutra EH, Nanda R, Kumbar SG, et al. Injectable RANKL sustained release formulations to accelerate orthodontic tooth movement. Eur J Orthod. 2019.

21.   Dunn MD, Park CH, Kostenuik PJ, Kapila S, Giannobile WV. Local delivery of osteoprotegerin inhibits mechanically mediated bone modeling in orthodontic tooth movement. Bone. 2007;41(3):446-55.

22.   Fernandez-Gonzalez FJ, Canigral A, Lopez-Caballo JL, Brizuela A, Cobo T, de

Carlos F, et al. Recombinant osteoprotegerin effects during orthodontic movement in a rat model. Eur J Orthod. 2016;38(4):379-85.

23.   Sydorak I, Dang M, Baxter SJ, Halcomb M, Ma P, Kapila S, et al. Microsphere controlled drug delivery for local control of tooth movement. Eur J Orthod. 2019;41(1):1-8.

24.   Hadjidakis DJ, Androulakis, II. Bone remodeling. Ann N Y Acad Sci. 2006;1092:385-96.

25.   Hattner R, Epker BN, Frost HM. Suggested sequential mode of control of changes in cell behaviour in adult bone remodelling. Nature. 1965;206(983):489-90.

26.   Roberts WE, Huja S, Roberts JA. Bone modeling: biomechanics, molecular mechanisms, and clinical perspectives. Seminars in Orthodontics. 2004;10(2):123-61.

27.   Baloul SS. Osteoclastogenesis and Osteogenesis during Tooth Movement. Front Oral Biol. 2016;18:75-9.

28.   Kitaura H, Kimura K, Ishida M, Sugisawa H, Kohara H, Yoshimatsu M, et al. Effect of cytokines on osteoclast formation and bone resorption during mechanical force loading of the periodontal membrane. ScientificWorldJournal. 2014;2014:617032.

29.   Boyce BF, Xing L, Shakespeare W, Wang Y, Dalgarno D, Iuliucci J, et al. Regulation of bone remodeling and emerging breakthrough drugs for osteoporosis and osteolytic bone metastases. Kidney Int Suppl. 2003(85):S2-5.

30.   Verna C, Dalstra M, Melsen B. The rate and the type of orthodontic tooth movement is influenced by bone turnover in a rat model. Eur J Orthod. 2000;22(4):343-52.

31.   Kim CH, You L, Yellowley CE, Jacobs CR. Oscillatory fluid flow-induced shear stress decreases osteoclastogenesis through RANKL and OPG signaling. Bone. 2006;39(5):1043-7.

32.   Seeman E. Bone modeling and remodeling. Crit Rev Eukaryot Gene Expr. 2009;19(3):219-33.

33.   Boyce BF, Xing L. Biology of RANK, RANKL, and osteoprotegerin. Arthritis Res Ther. 2007;9 Suppl 1:S1.

34.   Martin TJ, Sims NA. Osteoclast-derived activity in the coupling of bone formation to resorption. Trends Mol Med. 2005;11(2):76-81.

35.   Phan TC, Xu J, Zheng MH. Interaction between osteoblast and osteoclast: impact in bone disease. Histol Histopathol. 2004;19(4):1325-44.

36.   Lu J, Duan Y, Zhang M, Wu M, Wang Y. Expression of Wnt3a, Wnt10b, beta-catenin and DKK1 in periodontium during orthodontic tooth movement in rats. Acta Odontol Scand. 2016;74(3):217-23.

37.   Henneman S, Von den Hoff JW, Maltha JC. Mechanobiology of tooth movement. Eur J Orthod. 2008;30(3):299-306.

38.   Arnett TR, Gibbons DC, Utting JC, Orriss IR, Hoebertz A, Rosendaal M, et al. Hypoxia is a major stimulator of osteoclast formation and bone resorption. J Cell Physiol. 2003;196(1):2-8.

39.   Park HJ, Baek KH, Lee HL, Kwon A, Hwang HR, Qadir AS, et al. Hypoxia inducible factor-1alpha directly induces the expression of receptor activator of nuclear factor-kappaB ligand in periodontal ligament fibroblasts. Mol Cells. 2011;31(6):573-8.

40.   Li ML, Yi J, Yang Y, Zhang X, Zheng W, Li Y, et al. Compression and hypoxia play independent roles while having combinative effects in the osteoclastogenesis induced by periodontal ligament cells. Angle Orthod. 2016;86(1):66-73.

41.   Kobayashi Y, Hashimoto F, Miyamoto H, Kanaoka K, Miyazaki-Kawashita Y, Nakashima T, et al. Force-induced osteoclast apoptosis in vivo is accompanied by elevation in transforming growth factor beta and osteoprotegerin expression. J Bone Miner Res. 2000;15(10):1924-34.

42.   Taddei SR, Andrade I, Jr., Queiroz-Junior CM, Garlet TP, Garlet GP, Cunha Fde Q, et al. Role of CCR2 in orthodontic tooth movement. Am J Orthod Dentofacial Orthop. 2012;141(2):153-60.

43.   Taddei SR, Moura AP, Andrade I, Jr., Garlet GP, Garlet TP, Teixeira MM, et al. Experimental model of tooth movement in mice: a standardized protocol for studying bone remodeling under compression and tensile strains. J Biomech. 2012;45(16):2729-35.

44.   Tripuwabhrut P, Mustafa M, Gjerde CG, Brudvik P, Mustafa K. Effect of compressive force on human osteoblast-like cells and bone remodelling: an in vitro study. Arch Oral Biol. 2013;58(7):826-36.

45.   Zhang L, Liu W, Zhao J, Ma X, Shen L, Zhang Y, et al. Mechanical stress

regulates osteogenic differentiation and RANKL/OPG ratio in periodontal ligament stem cells by the Wnt/beta-catenin pathway. Biochim Biophys Acta. 2016;1860(10):2211-9.

46.   Hosomichi J, Shibutani N, Yamaguchi H, Hatano K, Kuma Y, Suzuki T, et al. Localization of leucine-rich repeat-containing G-protein-coupled receptor 5- and Ki67-positive periodontal cells expressing runt-related transcription factor 2 during tooth movement. Orthodontic Waves. 2018;77(4):197-208.

47.   Ghayor C, Correro RM, Lange K, Karfeld-Sulzer LS, Gratz KW, Weber FE. Inhibition of osteoclast differentiation and bone resorption by N-methylpyrrolidone. J Biol Chem. 2011;286(27):24458-66.

48.   Ratajczak MZ, Zuba-Surma E, Kucia M, Reca R, Wojakowski W, Ratajczak J. The pleiotropic effects of the SDF-1-CXCR4 axis in organogenesis, regeneration and tumorigenesis. Leukemia. 2006;20(11):1915-24.

49.   Ceradini DJ, Kulkarni AR, Callaghan MJ, Tepper OM, Bastidas N, Kleinman ME, et al. Progenitor cell trafficking is regulated by hypoxic gradients through HIF-1 induction of SDF-1. Nat Med. 2004;10(8):858-64.

50.   Kaku M, Kitami M, Rosales Rocabado JM, Ida T, Akiba Y, Uoshima K. Recruitment of bone marrow-derived cells to the periodontal ligament via the stromal cell-derived factor-1/C-X-C chemokine receptor type 4 axis. J Periodontal Res. 2017;52(4):686-94.

51.   De Clercq E. The AMD3100 story: the path to the discovery of a stem cell mobilizer (Mozobil). Biochem Pharmacol. 2009;77(11):1655-64.

52.   Meeson R, Sanghani-Keri A, Coathup M, Blunn G. VEGF with AMD3100 endogenously mobilizes mesenchymal stem cells and improves fracture healing. J Orthop Res. 2018.

53.   Toupadakis CA, Granick JL, Sagy M, Wong A, Ghassemi E, Chung DJ, et al. Mobilization of endogenous stem cell populations enhances fracture healing in a murine femoral fracture model. Cytotherapy. 2013;15(9):1136-47.

54.   Devine SM, Flomenberg N, Vesole DH, Liesveld J, Weisdorf D, Badel K, et al. Rapid mobilization of CD34+ cells following administration of the CXCR4 antagonist AMD3100 to patients with multiple myeloma and non-Hodgkin's lymphoma. J Clin Oncol. 2004;22(6):1095-102.

55.   Usumi-Fujita R, Hosomichi J, Ono N, Shibutani N, Kaneko S, Shimizu Y, et al.

Occlusal hypofunction causes periodontal atrophy and VEGF/VEGFR inhibition in tooth movement. Angle Orthod. 2013;83(1):48-56.

56.   Xu J, Chen Y, Liu Y, Zhang J, Kang Q, Ho K, et al. Effect of SDF-1/Cxcr4 Signaling Antagonist AMD3100 on Bone Mineralization in Distraction Osteogenesis. Calcif Tissue Int. 2017;100(6):641-52.

57.   Shimizu Y, Ishida T, Hosomichi J, Kaneko S, Hatano K, Ono T. Soft diet causes greater alveolar osteopenia in the mandible than in the maxilla. Arch Oral Biol. 2013;58(8):907-11.

58.   Kawamoto T. Use of a new adhesive film for the preparation of multi-purpose fresh-frozen sections from hard tissues, whole-animals, insects and plants. Arch Histol Cytol. 2003;66(2):123-43.

59.   Machado CC, Nojima Mda C, Rodrigues e Silva PM, Mandarim-de-Lacerda CA. Histomorphometric study of the periodontal ligament in the initial period of orthodontic movement in Wistar rats with induced allergic asthma. Am J Orthod Dentofacial Orthop. 2012;142(3):333-8.

60.   Dai Q, Zhou S, Zhang P, Ma X, Ha N, Yang X, et al. Force-induced increased osteogenesis enables accelerated orthodontic tooth movement in ovariectomized rats. Sci Rep. 2017;7(1):3906.

61.   Dai QG, Zhang P, Wu YQ, Ma XH, Pang J, Jiang LY, et al. Ovariectomy induces osteoporosis in the maxillary alveolar bone: an in vivo micro-CT and histomorphometric analysis in rats. Oral Dis. 2014;20(5):514-20.

62.   Ren Y, Maltha JC, Kuijpers-Jagtman AM. The rat as a model for orthodontic tooth movement--a critical review and a proposed solution. Eur J Orthod. 2004;26(5):483-90.

63.   Liu X, Zhou C, Li Y, Ji Y, Xu G, Wang X, et al. SDF-1 promotes endochondral bone repair during fracture healing at the traumatic brain injury condition. PLoS One. 2013;8(1):e54077.

64.   Liu C, Weng Y, Yuan T, Zhang H, Bai H, Li B, et al. CXCL12/CXCR4 signal axis plays an important role in mediating bone morphogenetic protein 9-induced osteogenic differentiation of mesenchymal stem cells. Int J Med Sci. 2013;10(9):1181-92.

65.   Petit I, Jin D, Rafii S. The SDF-1-CXCR4 signaling pathway: a molecular hub

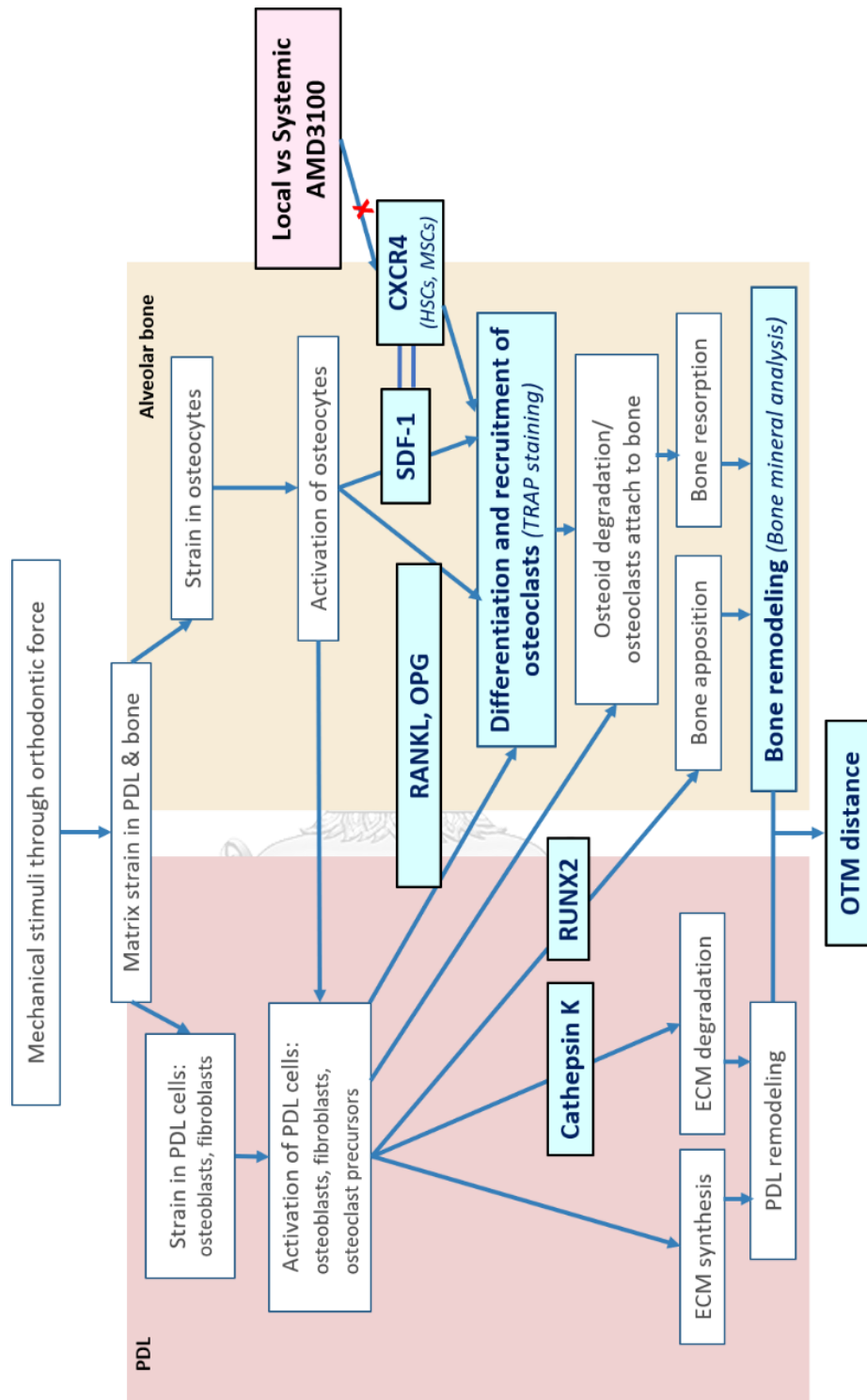modulating neo-angiogenesis. Trends Immunol. 2007;28(7):299-307.
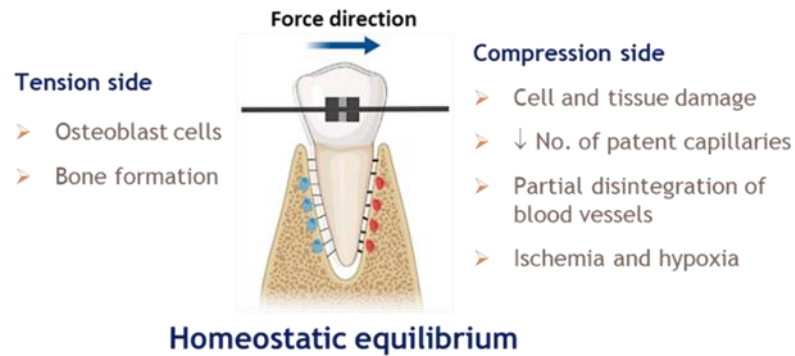
Figure 1 Conceptual framework

Figure 2 Homeostatic equilibrium during orthodontic tooth movement
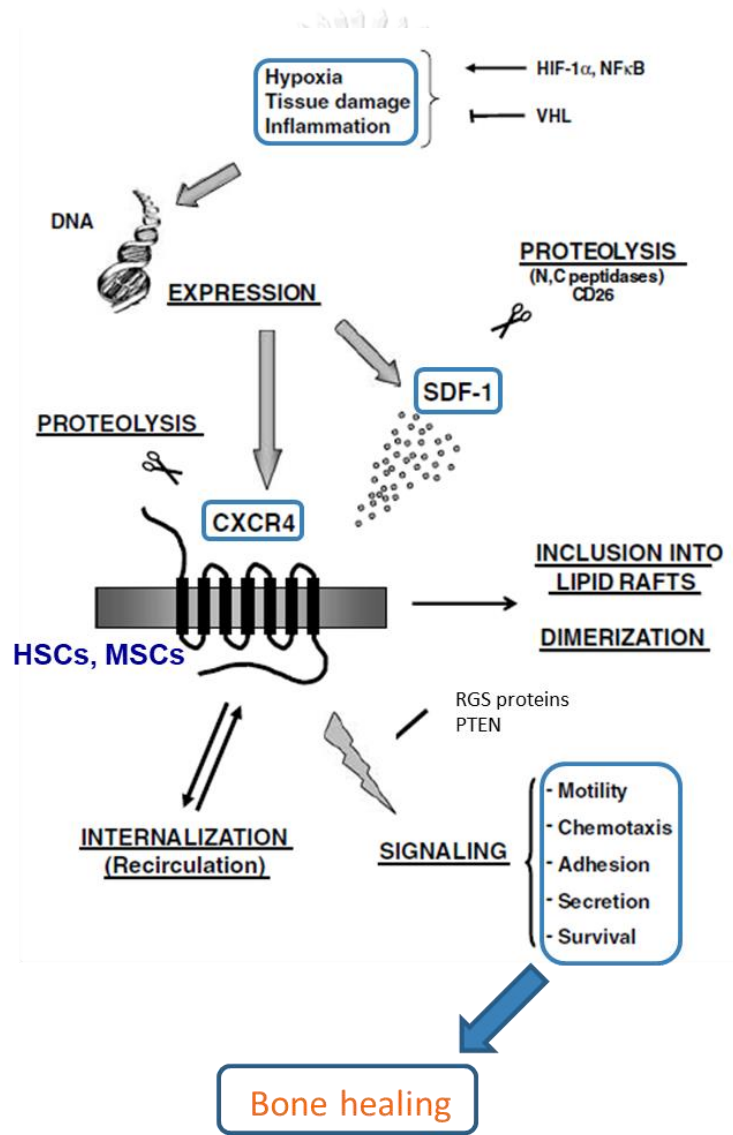

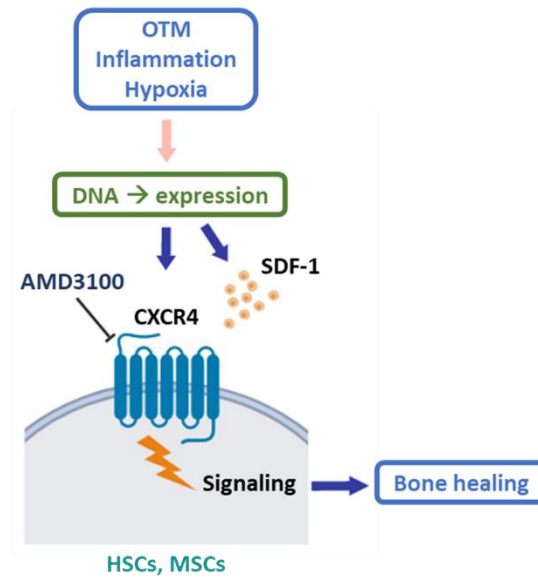*Figure 3* Diagram shows the different levels of regulation of SDF-1/CXCR4 axis

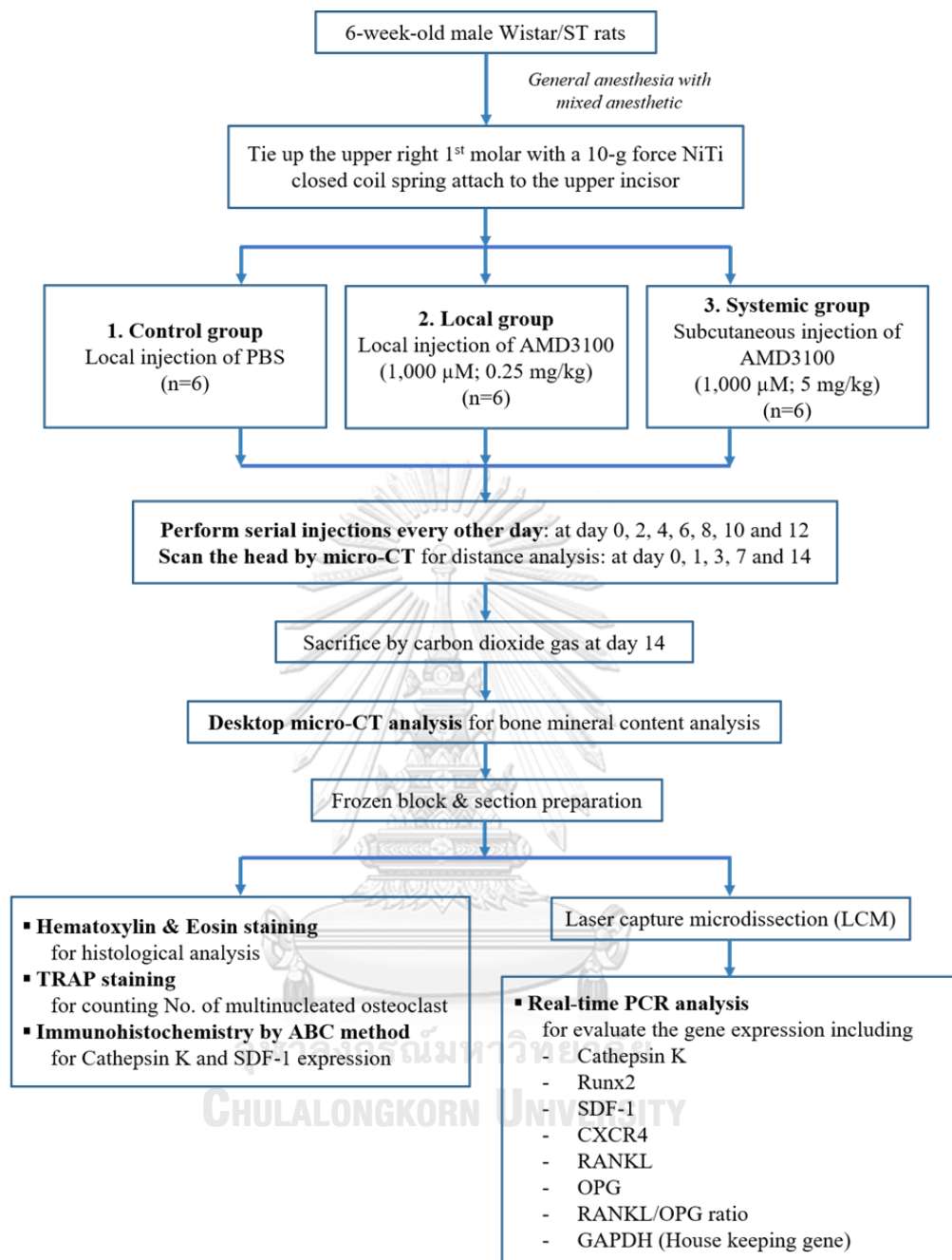*Figure 4* Schematic diagram expresses the strategy to target the SDF-1/CXCR4 axis
using AMD3100
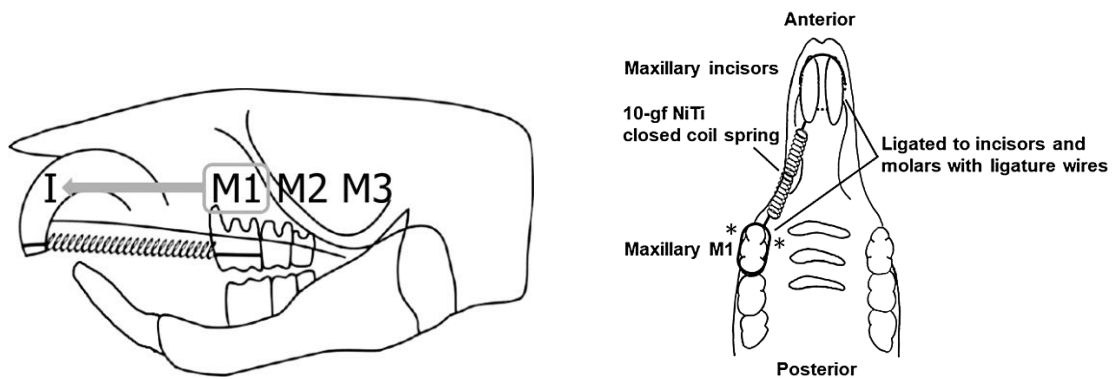
Figure 5 Diagram of research methods

Figure 6 Schematic illustration of the rat orthodontic tooth movement model. A 10-gf NiTi closed coil spring is attached to the right maxillary M1 and the maxillary incisors to move right M1 mesially. (I, maxillary incisors; M1, first molar; M2, second molar; M3, third molar; *, local injection area)
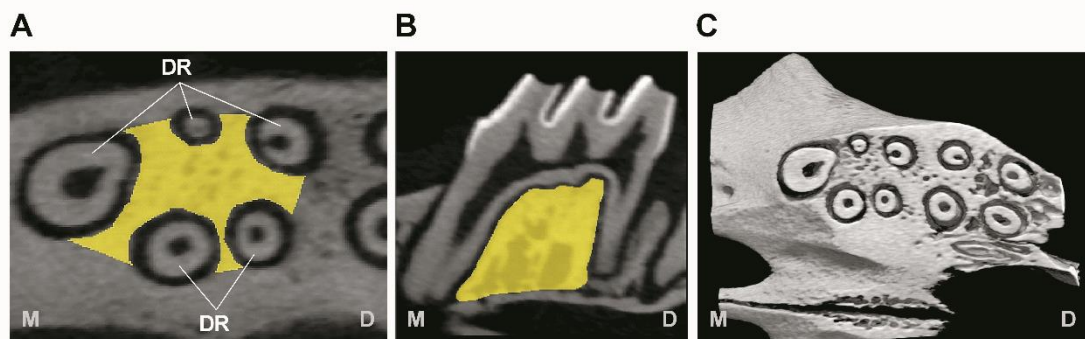
Figure 7 Three-dimensional micro-CT images show region of interest (ROI) for bone analysis. (A) Horizontal section; (B) sagittal section of the interradicular alveolar bone of the maxillary right M1. The ROI (yellow) was defined as the interradicular septal bone among the dental roots of M1. (C) Morphology of the interradicular septal bone in the maxillary right M1 and M2 region. M, mesial; D, distal; DR, dental root.
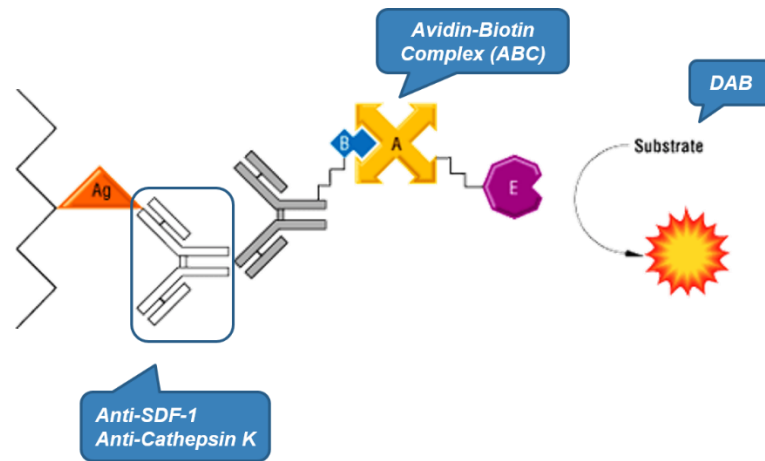
Figure 8 Immunohistochemical analysis by ABC method using DAB as a visualized substrate for the detection of cathepsin K and SDF-1 expressions in the PDL tissue
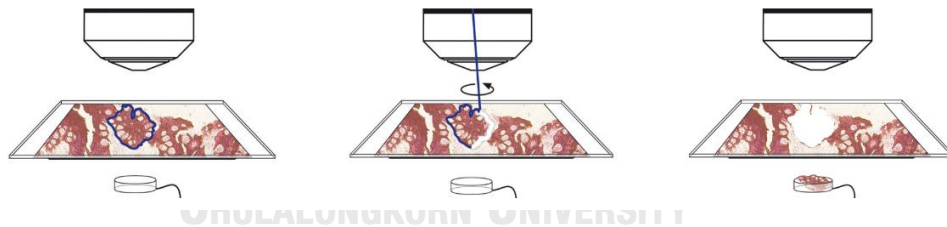

Figure 9 Laser capture microdissection method for collecting PDL tissue from the compression side of mesial root of M1
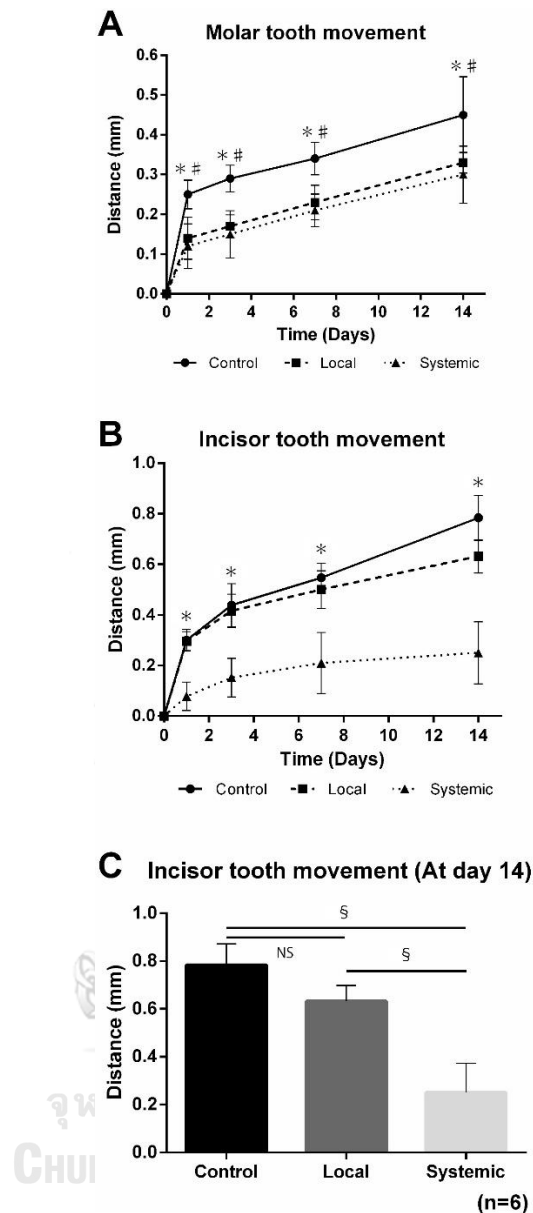
Figure 10 Serial local administration of AMD3100 inhibits molar but not incisor movement. (A) The maxillary M1 movement in local and systemic groups treated with AMD3100 significantly decreased on d 1, 3, 7, and 14 after applying mechanical loading compared with the control group. *P <0.05 local vs the control group. #P <0.05 systemic vs the control group. (B) Total distal incisor movement. There was no significant difference in incisor retraction between the group with serial local administration of AMD3100 and the control group.
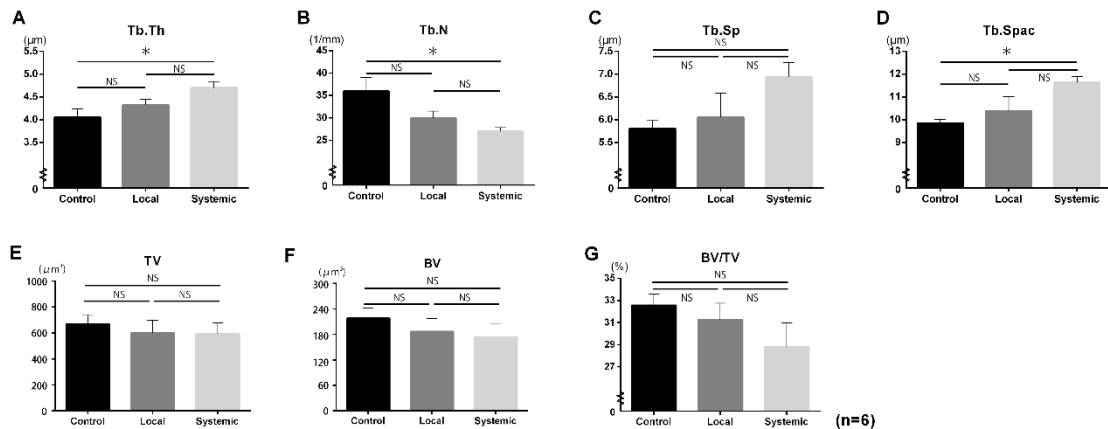
Figure 11 Micro-CT data showing the following: (A) Tb.Th; (B) Tb.N; (C) Tb.Sp; (D) Tb.Spac; (E) TV; (F) mineralized BV; and (G) BV/TV in the interradicular alveolar bone ROI of maxillary M1. Each point represents the mean ± SD; n = 6; *P <0.05.
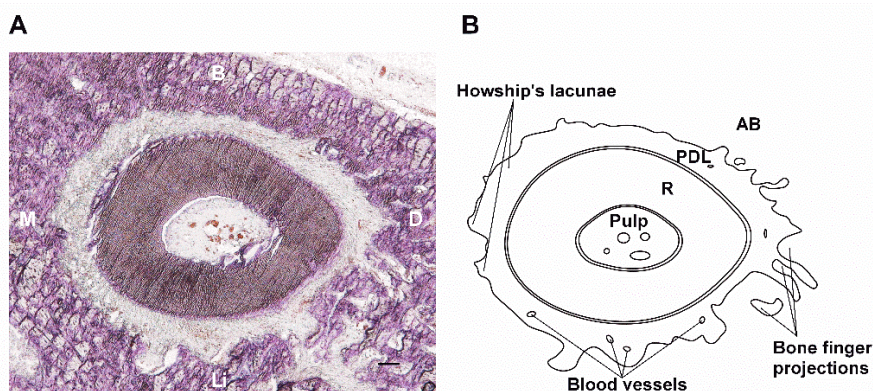

Figure 12 Histological and schematic observation (A) Histological images of hematoxylin and eosin staining of the medial root of the maxillary first molar (M1) and (B) schematic representation. On the compression side, Howship's lacunae were observed on the bone surface facing the PDL. On the tensile side, bone finger projections, stretched collagen fibers and blood vessels were observed. AB, alveolar bone; PDL, periodontal ligament; R, tooth root; M, mesial; D, distal; B, buccal; L, lingual. Scale bars = 100 μm.
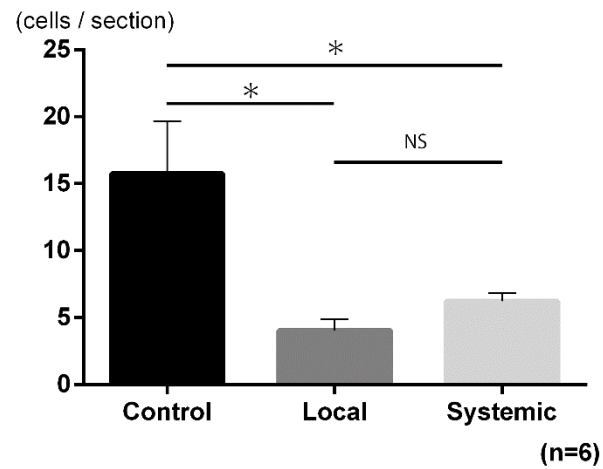
Number of TRAP-positive multinucleated cells

Figure 13 The numbers of TRAP-positive multinucleated osteoclasts in the PDL around the mesial root of M1 on d 14. In the local and systemic administration groups treated with AMD3100, the TRAP-positive osteoclasts were significantly decreased after mechanical loading compared with the control group. There was no difference in osteoclasts between local and systemic groups after OTM. Each point represents the mean ± SD; n = 6; *P <0.05.
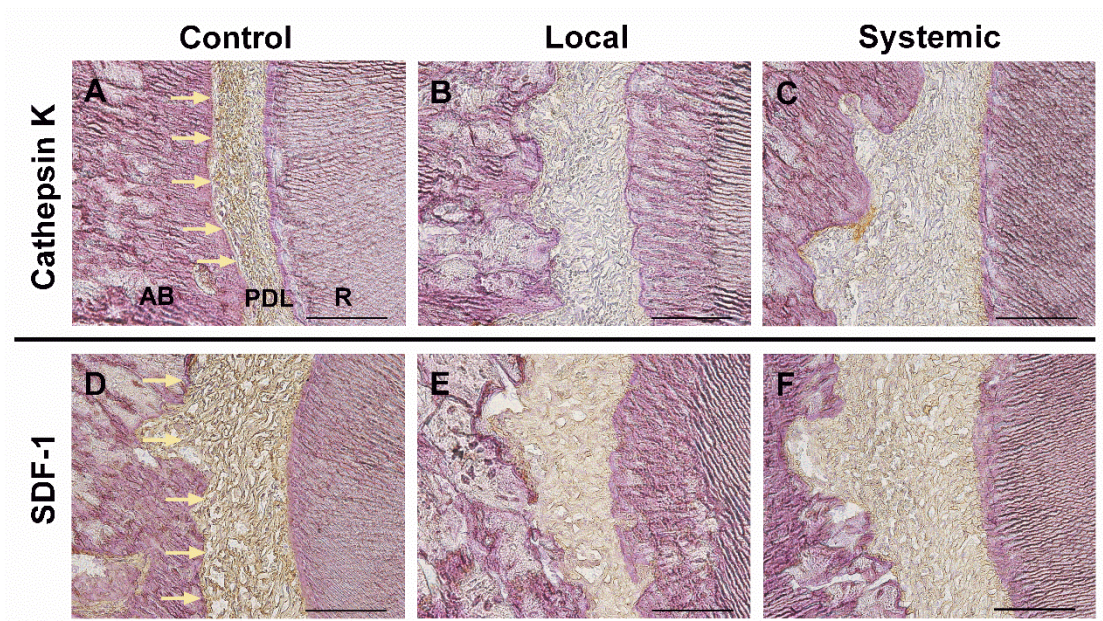
Figure 14 Immunohistochemical detection of cathepsin K and SDF-1 to indicate the contribution of osteoclastic activity and the SDF-1/CXCR4 axis, respectively. The regions of interest were on the compression side of the alveolar bone and the PDL of the control, local, and systemic groups. Cathepsin K (A-C) and SDF-1 (D-F) -positive dark brown cells were observed in the extracellular matrix of the PDL only in the control group (A and D; yellow). In the cathepsin K target, slightly positive cells were indicated in the systemic group (C) but were absent in the local group (B). Few SDF-1 positive cells were similarly observed for the local (E) and the systemic groups (F). AB, alveolar bone; R, tooth root; M, mesial; D, distal; B, buccal; L, lingual. Scale bars = 100 μm.
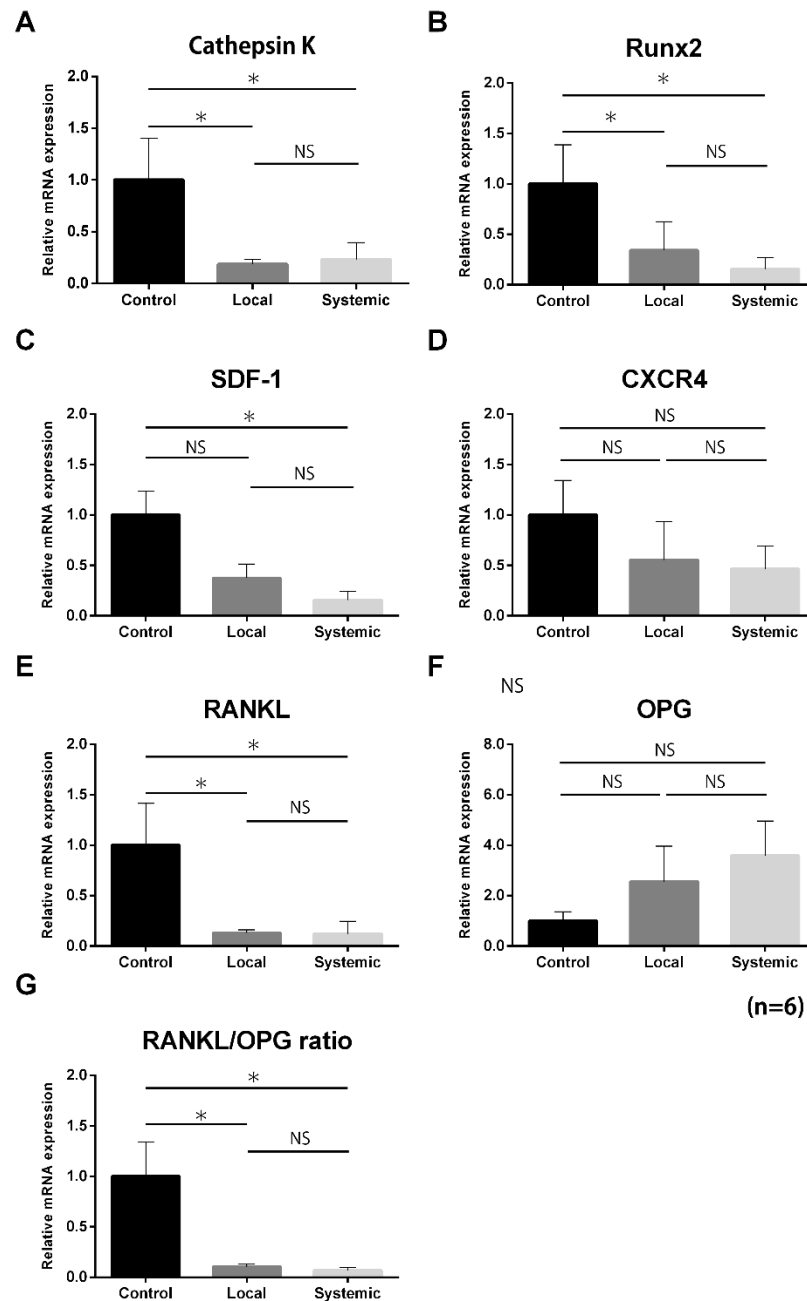
Figure 15 Evaluation of the expression of key genes involved in osteoclast precursors, osteogenesis, and the SDF-1/CXCR4 axis. The relative mRNA expression levels of the following: (A) cathepsin K; (B) Runx2; (C) SDF-1; (D) CXCR4; (E) RANKL; (F) OPG; and (G) RANKL/OPG ratio within the PDL of the mesial root of maxillary M1 were determined at d 14 of tooth movement. The results are expressed as the mean ± SD of relative mRNA levels; n = 6; *P <0.05.

VITA

NAME   Narubhorn Ongprakobkul

DATE OF BIRTH   10 July 1989

PLACE OF BIRTH   Bangkok

INSTITUTIONS ATTENDED   Chulalongkorn University

HOME ADDRESS   134 Ladpraw 124, Plubpla, Wangthonglang, Bangkok 10310

PUBLICATION   Ongprakobkul N, Ishida Y, Hatano-Sato K, Li K, Petdachai S, Usumi-Fujita R, et al. Effects of local vs systemic administration of CXCR4 inhibitor AMD3100 on orthodontic tooth movement in rats. Am J Orthod Dentofacial Orthop. 2022.

Li K, Ishida Y, Hatano-Sato K, Ongprakobkul N, Hosomichi J, Usumi-Fujita R, et al. Nuclear factor-kappa B decoy oligodeoxynucleotide-loaded poly lactic-co-glycolic acid nanospheres promote periodontal tissue healing after tooth replantation in rats. J Periodontol. 2022;93(3):458-70.

Suwanwela J, Nitipong V, Ongprakobkul N. Single nucleotide polymorphisms associated with Angle's Class I and III occlusal relationship in Thais with thyrotoxic hypokalemic periodic paralysis. CU Dent J. 2015;38:185-96.